Blind Inference of Nonlinear Cable Network Topology from Sparse Data

Vic Anand, Hod Lipson, Francisco Valero-Cuevas
Sibley School of Mechanical and Aerospace Engineering
Cornell University, Ithaca, NY 14853, USA
+1 (607) 255-0581
{vic.anand, hod.lipson, fv24}@cornell.edu

ABSTRACT

We demonstrate a method to infer the topology of a hidden nonlinear network of cable-like links (elements that can sustain only tensile loads) given limited data on the hidden network. The hidden networks are based on two classical representations of the tendon network of a human finger, containing 11 and 16 links, respectively. The phenotype consists of a regular, mesh-like network of 72 links whose properties are modified by our evolutionary algorithm. Using 30 data points, randomly obtained from the hidden network, we evolved networks whose functional behavior reproduced that of the hidden network, and whose topology closely matched that of the hidden network.

1. INTRODUCTION

We are interested in extracting the structure of hidden systems whose behavior is observable only through observations of inputs and outputs; systems of this type are commonly referred to as "black box". The process of developing of a model for a system given input and output data is known as system identification.

Identification of a nonlinear system can be a difficult problem. The difficulty of this problem increases as the number of observations permitted on the hidden system and the number of *a priori* modeling assumptions allowed are reduced.

Numerous methods exist for identification of linear [9][10] and nonlinear [8] systems. Neural networks and fuzzy systems are commonly used to identify nonlinear systems [8]. In the field of system biology, the problem of genetic network inference has received much attention; this is a nonlinear system identification problem in which the structure of a network is sought. Myriad methods, such as Bayesian network inference algorithms [11], simulated annealing [11], clustering [3], and evolutionary algorithms [1][5], have been employed in this problem.

A limitation of some nonlinear system identification methods, such as neural networks, is that the resulting models mathematically map inputs to outputs but provide little insight into system function. Another limitation is that some methods, such as Bayesian networks, infer correlation but not causality.

In contrast, we seek *functional* models that provide insight into the system's inner workings. For example, a functional model of a mechanical structure describes the components of that structure, as well as their layout and parameters. This type of model thus allows its user to gain insight into the effects of changes on the system being modeled.

In this work, we limit our systems of interest to networks of cables, which are inherently nonlinear. Since cables can sustain only tensile loads, their force-length relationship is nonlinear. Thus, depending on the layout and loading of the network, some cables may carry no load, rendering those cables unobservable under that particular loading condition.

We also seek to perform system identification using limited, sparse data. For some systems, such as biological systems, only limited data can be obtained. Also, the properties of the system may change with time, adding additional dimensionality to the problem. Thus, methods that can perform system identification with sparse data are desirable for certain classes of problems.

We use a genetic algorithm (GA) to evolve virtual networks of cables whose functional behavior is identical to that of a virtual target network of cables. The target network is hidden from the genetic algorithm because the fitness of individuals in the GA depends only on the inputs and outputs of the target network; the individuals have no knowledge of the target system's structure or internal state.

Our inference method alternates between testing of the target system and evolution of new networks. After a test (a set of inputs and the resulting outputs) is performed on the hidden network, the GA evolves networks to explain that *and all previous tests*. Since we seek to reduce the number of tests on the target system, this method allows us to observe the performance of the evolved networks after each test and decide whether to stop. It also provides the opportunity to design new tests based on the performance of the GA during previous tests. By contrast, a method that performs batch testing on the target system may unnecessarily tax the target system if some tests uncover little new information. Also, previous research suggests that presentation of a batch of data to the GA may overwhelm it, increasing the time needed to evolve good networks [2].

GECCO '05, June, 2005, Washington, DC, USA.

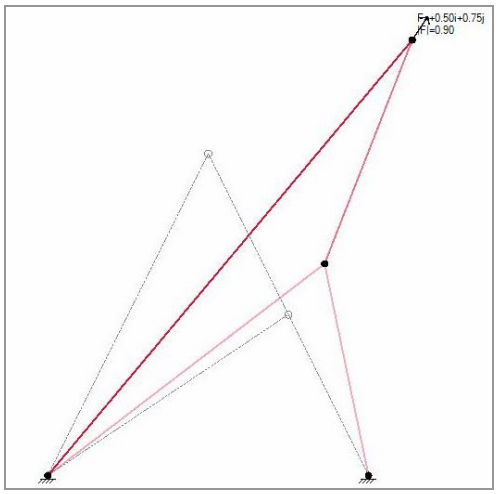

Figure 1. A network that resembles the letter 'A'. The bottom nodes are grounded. Gray lines show the un-stretched configuration and red lines show the network under an arbitrary loading condition. The shade of red indicates the level of tension in the link, with dark red indicating higher tension.

Individuals in our GA are square meshes (Figure 3); the evolutionary process modifies the resting (free) lengths of cables in the individuals, thereby changing the functional behavior of the network. We hypothesize that a mesh can be morphed into a network whose functional behavior is similar to that of another less complicated network. This idea was inspired by biology: in mammals, *in utero* skeletal structures are sheets of cartilage. As loads are applied, sections of the sheet that bear the load harden into bones [4]. By analogy, in our virtual meshes, a cable can shortened to amplify its role in the network, or lengthened to decrease its role; if sufficiently long, that cable may never bear tension under admissible loading conditions.

The resulting evolved networks exhibit functional behaviors that reproduce those of their target hidden networks. In addition, they display topologies that closely resemble those of their target hidden networks.

Ultimately, we plan to extend this work to nonlinear biological structures, such as the tendon network of a finger. For that reason we chose to work with cables that, like tendons, are unable to sustain compressive loads.

2. METHODS

In this work, we infer the topology of a hidden network of cables. The hidden network is a virtual, i.e. simulated, network.

2.1 Network Modeling Assumptions

A network is a planar, two-dimensional entity consisting of a set of massless cables, or links, connected by frictionless, massless hinges, or nodes (see Figure 1). At any node, the cables connected to it can freely rotate about the node, independent of the other cables. Every link is connected to exactly two nodes. Overlapping links incur no frictional penalty and no additional length due to routing. One or more nodes in the network must be grounded, such that their position remains fixed regardless of the force applied at the node. Externally applied forces, resolved into horizontal and vertical components, can be applied at any ungrounded node.

The constitutive relationship for a link is defined to be:

$$F = \begin{cases} \frac{E \cdot A}{l_0}(l - l_0), & l \geq l_0 \\ 0, & l < l_0 \end{cases}$$

where F is the force exerted by a link on its end nodes, E the elastic modulus, A the cross-sectional area, l_0 the resting length of the link, and l the current length of the link. If l is less than or equal to l_0, the link exerts no force on its end nodes. In this work, we set E and A to 1.0, and did not change them. Since, for any given link, l_0 is also a constant, the links exhibit linear force-length behavior in tension, and are slack otherwise.

2.2 Finding Network Static Equilibrium

Given a network and one or more applied external forces, it was necessary to determine the final static equilibrium configuration of the network. This was accomplished using a relaxation method [6] that works as follows. At every node, calculate the residual force, which is the sum of the forces applied by links and the external forces. Displace the node in the direction of the residual force. Repeat until residual force on ungrounded nodes approaches zero within the desired accuracy. This method is detailed below:

1. For every link
   a. Calculate tension based on the positions of the link's end nodes; those positions determine the length of the link, and hence its tension can be calculated from its force-length function.
   b. Increment the residual force at each end node of the link by the tension calculated in the previous step.
2. For every node
   a. Add any external force applied at the node to the residual force calculated in step 1 to obtain net force
   b. Calculate node stiffness (a sum of the stiffness of all links connected to that node)
   c. Displace node by $\alpha \times F/S$ in the direction of F, where F is the net force at the node, S is the node stiffness, and α is a relaxation factor in the range $0<\alpha<1$.
3. Calculate network error, $E \equiv \max(R)$, where R is the set of residual forces of all the ungrounded nodes.
4. Repeat steps 1-3 until $E \leq \varepsilon$, where E is the network error and ε is the desired accuracy

This method is guaranteed to converge if at least one node is grounded and if the links possess a monotonic force-length function. See reference [6] for details.

2.3 Method to Infer Hidden Network

The problem of cable network inference is one of system identification with sparse data. The data is obtained through testing of the target system. A test is defined as a set of forces applied at pre-specified nodes on the target network. Those forces are applied and the target network is relaxed using the

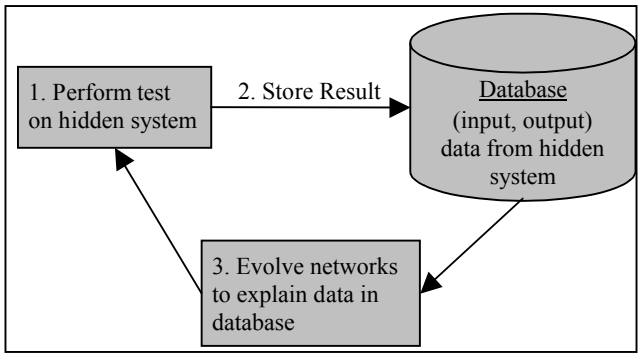

Figure 2. Method to infer hidden network structure

method described in section 2.2. The set of residual forces remaining at the grounded nodes are the outputs.

A data point therefore consists of a set of input forces and a set of output forces recorded at the grounded nodes. In the example shown in Figure 1, a sole input force is applied at the topmost node. The residual forces recorded at the bottom grounded nodes after relaxing the network constitute the output.

Testing of the hidden system and evolution of new networks are alternated. A test is performed on the hidden system and its result stored in a database. Networks are then evolved to explain that test *and all previous tests in the database*. The process repeats until a pre-specified number of tests have been performed on the hidden system. The pseudo-code for this is shown below (see also Figure 2):

```
For t = 1..n
    Perform test t on hidden network and record its I/O data
    Create a population of individuals
        Seed the population with the best 25% of the
        population from the previous iteration
        Fill the remaining population with random individuals
        Calculate individual fitness based on tests 1 to t
    Evolve the population until the maximum fitness reaches
    a plateau
End
```

Here n is the number of tests to be performed on the hidden system. Note that during iteration t, the individuals evolved must explain *all* previous data points, 1..t.

2.4 Genetic Encoding of the Network

In the genetic algorithm, each individual is a network of 25 nodes, arranged in a regular 5x5 layout, and 72 horizontal, vertical, and diagonal links. Thus, the individuals resemble a mesh (see Figure 3). A direct encoding is used; the genotype and phenotype are the same. Depending on the problem, different nodes are grounded. In the example shown in Figure 3, the bottom left and right nodes are grounded. Cables only connect at circled nodes.

The dimensions of the GA individuals, as well as the positions of their input and grounded nodes, match those of the target network. If the target fits within a rectangle of dimension $n \times m$, of arbitrary length units, the mesh dimensions will also be $n \times m$. Also, input forces are applied to the same location in both the

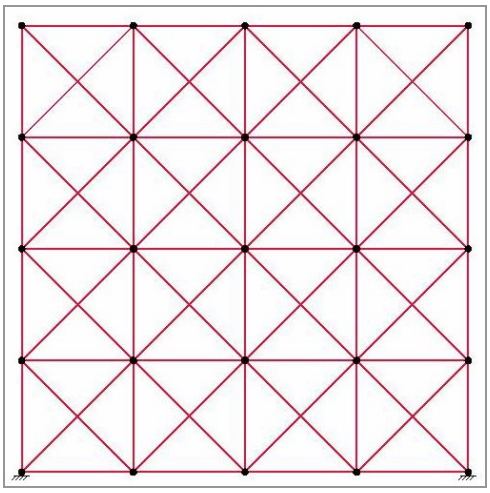

Figure 3. Genotype and phenotype used in the genetic algorithm. Cables only connect at circled nodes

target system and the meshes. If the target system has an input node at the Cartesian location (x, y), then the mesh, in its resting configuration, must have a node at (x, y) at which an input force can be applied. Finally, if the target system has a grounded node at location (x', y'), then the GA individuals must also have a grounded node at the same location.

The behavior of the network depends upon the resting (free) lengths of the links, and the location of the grounded nodes. In any particular problem, the set of grounded nodes remains constant, as do the values of E and A, the elastic modulus and cross-sectional area of the links. Thus, the functional behavior of the network is determined entirely by the resting lengths of the links in the network, and the genetic operators operate exclusively on these resting lengths.

2.4.1 Fitness

The fitness of an individual is a function of the error between the output predictions of the individual and the actual outputs observed from the target network. To calculate the fitness of an individual in the GA population, the data obtained from the target system are used. Each data point has the form:

$$\left(\{F_{i1}, F_{i2}, \ldots, F_{im}\}, \{F_{o1}, F_{o2}, \ldots, F_{on}\}\right)$$

where the F_i's are input forces applied to the target network and the F_o's are the output forces observed at the grounded nodes.

The input forces from a data point are applied to the individual whose fitness is being calculated. That individual is then brought to its static equilibrium configuration using the relaxation method presented in section 2.2. The residual forces at the grounded nodes are then stored as:

$$\{F'_{o1}, F'_{o2}, \ldots, F'_{on}\}$$

Since the target network and the GA individuals have the same dimensions and identical locations of input and output nodes, the force outputs of a highly fit individual should match those of the target network. The difference between actual and predicted

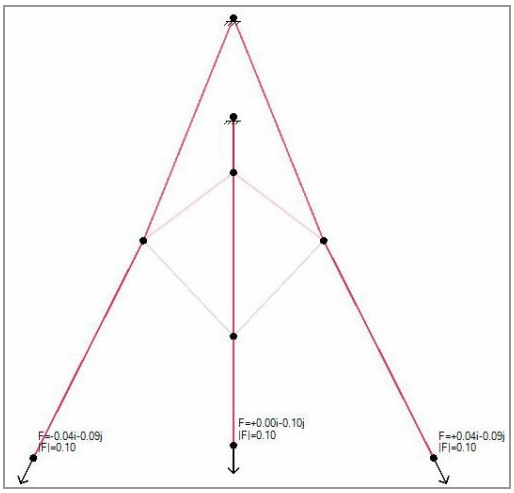

Figure 4. An implementation of Winslow's tendinuous rhombus. Red lines represent cables in tension, with dark red indicating higher tension. Gray lines represent slack cables. Note that in this particular loading configuration, two links are slack.

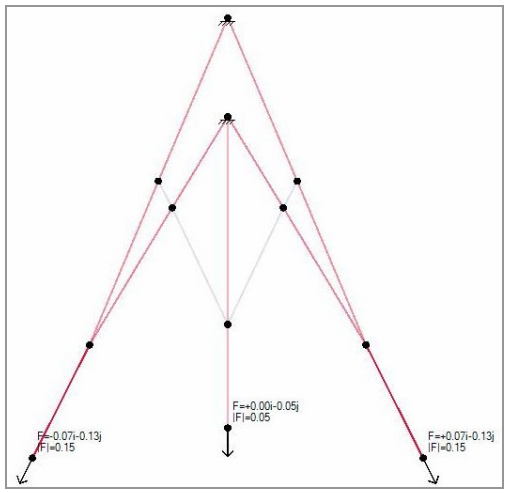

Figure 5. An alternative implantation of Winslow's tendinuous rhombus. In this particular loading configuration, four links are slack.

forces constitutes the error of the network for that data point. The error for data point p, ε_p, is given by:

$$\varepsilon_p = \sum_{j=1}^{n} \frac{\left|\overrightarrow{F'_{oj}} - \overrightarrow{F_{oj}}\right|}{\left|\overrightarrow{F_{oj}}\right|}$$

where n is the number of output (grounded) nodes in the network, F' is the force predicted by the GA individual, and F is the force observed in the target system. Note that the forces are vector quantities. Therefore, if F' and F have equal magnitude but different direction, the error will be nonzero. Also note that the error contribution from each output force is normalized.

The total error for the network is a weighted contribution of the average error and the maximum error calculated over all the data points.

$$\varepsilon_{total} = \frac{1}{2} \cdot \overline{\varepsilon_p} + \frac{1}{2} \cdot Max\left(\varepsilon_p\right)$$

The fitness is defined to be:

$$Fitness = 1.0 - \varepsilon_{total}$$

2.4.2 Genetic Operators

We chose deterministic crowding [7] as the selection method. The mutation operator performs point mutations by modifying the resting length of randomly chosen links in the network. The resting length of a link is incremented by a number drawn from a normal distribution with a mean of zero. We chose a two-dimensional crossover operator; it swaps all links in between two randomly chosen nodes of the parents.

2.5 Target Networks

We attempted to infer three different target networks. The first had a shape similar to that of the letter 'A' (Figure 1). In this network, the bottom two nodes are grounded and a force is applied to only the topmost node; the applied force is limited to one with an upward vertical component. The second and third target networks (Figures 4 and 5) are based on the Winslow's tendinuous rhombus [12], a classical description of the tendon network of a human finger dating from the 17th century. In these networks, the top two nodes, which lie along the vertical centerline of the network and correspond to tendon insertions into bone, are grounded.

External forces are applied to the bottom three nodes; these forces are parallel to the input tendons in their resting configuration and their vertical components are required to be downward. Additionally, the force magnitudes are capped.

For the 'A', a total of nine tests was run on this network: applied force magnitudes of 0.5, 1.0, and 1.5 with angles of 45°, 90°, and 135°, with the angle measured from the positive x-axis. After a test, networks were evolved to explain that test and all previous tests. The force magnitude was varied in an outer 'FOR' loop, and the angle varied in an inner 'FOR' loop.

For the Winslow rhombuses, thirty random tests were generated. Since the angles of the applied external forces constrained to be parallel to the input tendons and downward, a test consisted of a set of three force magnitudes. After each randomly generated test, networks were evolved to explain that test and all previous tests.

3. RESULTS

3.1 Evolving an 'A'

We evolved a network whose functional behavior and topology resembled the 'A' of Figure 6d. Figures 6a-c show the evolution of the network. With only one data point, the genetic algorithm was not able to evolve a network whose topology resembled that of the target system. However, after only three tests on the target system, evolution found a network whose topology resembled the 'A' of Figure 6d. Notice that the network in Figure 6b displays a kink on the right that is characteristic of the 'A' when pulled up and to the right. Also note that the distribution of tensions in the

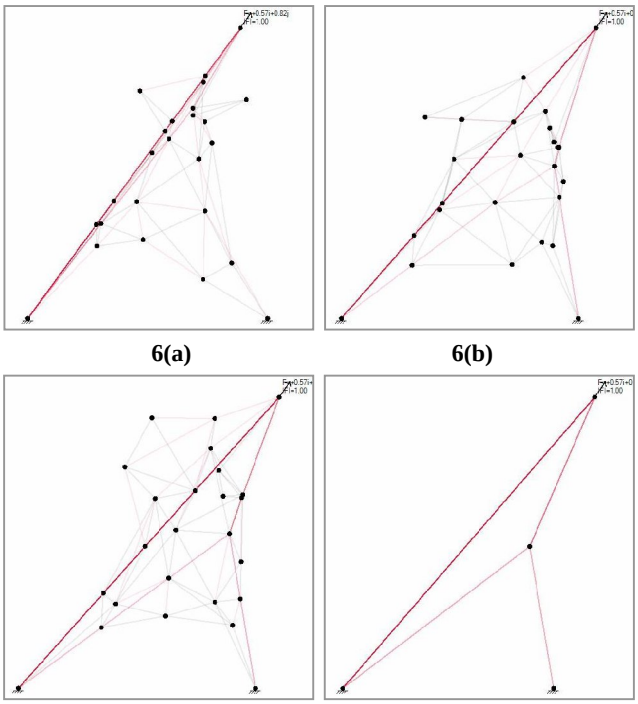

6(a) 6(b)

6(c) 6(d)

Figure 6. Evolution of an 'A'. Figure 6(a)-(c) show the best network evolved after 1, 3, and 9 tests, respectively, on the target network. 6(d) shows the target network.

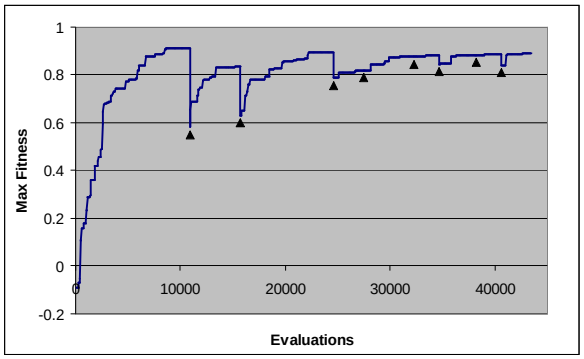

Figure 7. The maximum fitness of the population vs. the number of individuals evaluated for the 'A' network. Markers indicate a new test performed on the target system.

networks of Figures 6b and 6c are similar to that of the target network.

Figure 7 shows the maximum fitness of the GA population versus the number of individuals evaluated for the 'A'. Markers indicate points where new tests were performed on the target system. Notice that the maximum fitness often drops at these points as new data is made available for fitness calculations. The fitness of the network shown in Figure 6(c), the best evolved using data from nine tests on the target system, was 0.89.

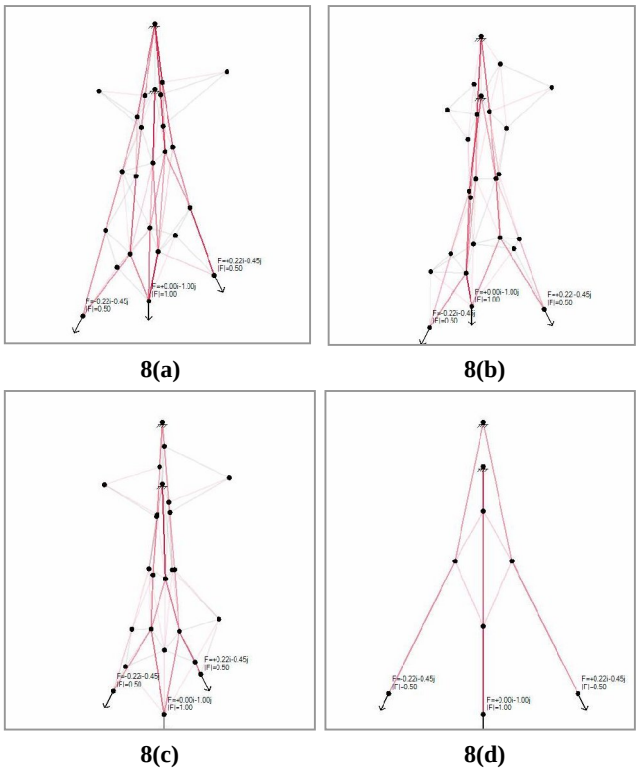

8(a) 8(b)

8(c) 8(d)

Figure 8. Evolution of a Winslow's rhombus. Figures 8(a)-(c) show the best network evolved after 1, 10 and 30 tests, respectively, on the target network. 8(d) shows the target network.

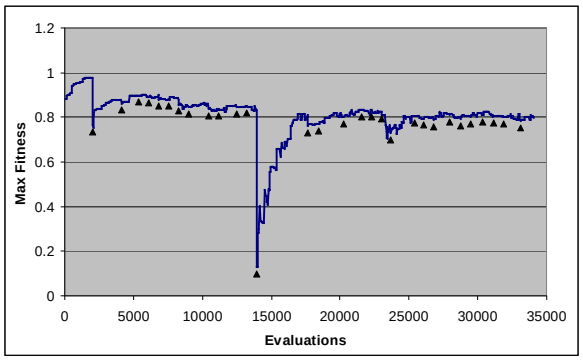

Figure 9. The maximum fitness of the population versus the number of individuals evaluated for the first Winslow's rhombus. Markers indicate a new test performed on the target system.

3.2 Evolving Winslow's Rhombus

We were able to evolve a network whose functional behavior and topology were similar to the Winslow's rhombus structure shown in Figure 8d. Figures 8a-c show the evolution of the network. With only one data point, the genetic algorithm was not able to evolve a network whose topology resembled that of the target system (Figure 8a). After ten tests on the target system, the topology of the best network began to resemble that of the target network as a rhombus began to emerge in the middle (Figure 8b). After thirty tests, a rhombus is clearly visible, and the network

appears symmetric about its vertical centerline (Figure 8c). Kinks in the outer tendons are visible, as they are in the target network. However, the center tendon in the target system that runs from the lower ground to the middle input node is not visible in the fully evolved network.

Figure 9 shows, for the evolution of the first Winslow's rhombus, the maximum fitness of the GA population versus the number of individuals evaluated. Markers indicate points where new tests were performed on the target system. Notice that while most tests caused a slight dip in fitness, one test caused a precipitous drop in the maximum fitness. The fitness of the network shown in Figure 8c, the best evolved using data from thirty tests on the target system, was 0.80.

3.3 Evolving another Winslow's Rhombus

We were able to evolve a network whose functional behavior and topology were similar to the alternate Winslow's rhombus structure shown in Figure 10d. Figures 10a-c show the evolution of the network. With only one data point, the genetic algorithm was able to find some of the topological features of the target network, such as the rhombus and the interconnections between the outer tendons and the rhombus (Figure 10a). After ten tests on the target system, the topology of the upper portion of the best network began to gel (Figure 10b). After thirty tests, the rhombus is clearly visible, and the network appears fairly symmetric about its vertical centerline (Figure 10c). There is also a clearer distinction between the outer tendons and the rhombus.

Figure 11 shows, for the evolution of the alternate Winslow's rhombus, the maximum fitness of the GA population versus the number of individuals evaluated. Markers indicate points where new tests were performed on the target system. Notice that while some tests caused a noticeable drop in fitness, many tests resulted in a slight increase of the population maximum fitness. Also note that the fitness never fully recovers from its initial drops, and plateaus below 0.8. The fitness of the network shown in Figure 10(c), the best evolved using data from thirty tests on the target system, was 0.78.

4. DISCUSSION

4.1 Observability and Network Equivalence

Observability and equivalence were two key issues in our minds at the inception of this work. A link is observable if the output of a target system cannot be explained unless that system contains the observable link. This issue is strongly related to that of equivalence – can networks with different topologies have equivalent functional behavior?

The 'A' network served as a test case for these issues. If the cross member is sufficiently long that it can never bear tension during admissible loading conditions then it is necessarily unobservable. However, if the cross member is not excessively long, and the network is pulled in a direction that elongates the cross member, it causes a kink in the right cable. That kink will alter the direction of the residual force at the right ground node. Can this alteration of the ground force be fully explained by a network that lacks the cross member?

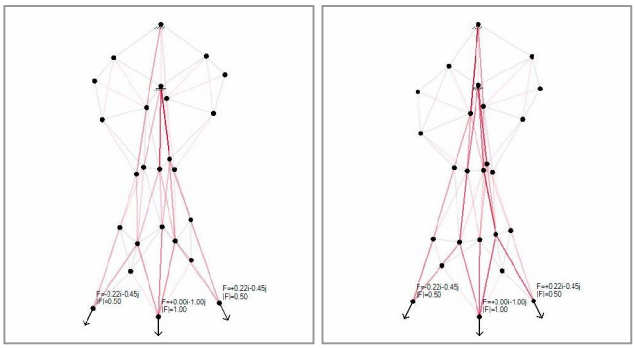

10(a) **10(b)**

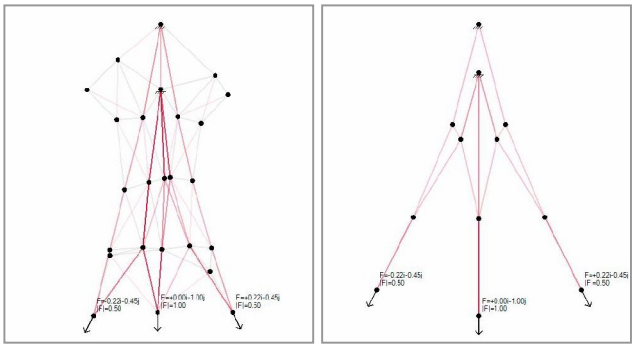

10(c) **10(d)**

Figure 10. Evolution of a different Winslow's rhombus. Figures 10(a)-(c) show the best network evolved after 1, 10, and 30 tests, respectively, on the target network. 10(d) shows the target network.

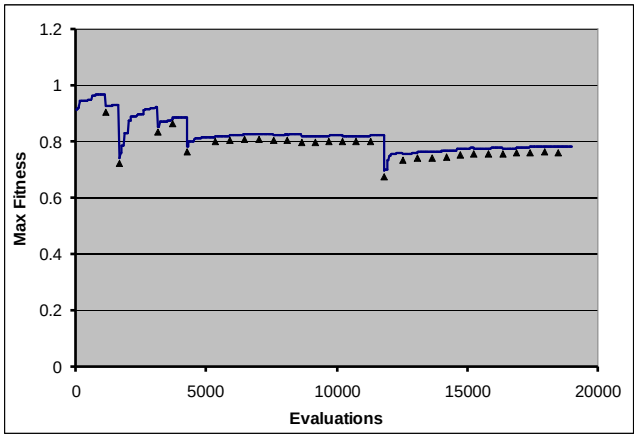

Figure 11. The maximum fitness of the population versus the number of individuals evaluated for the second Winslow's Rhombus. Markers indicate a new test performed on the target system.

In our tests, the genetic algorithm was not always able to evolve a network with a cross member. The resulting networks resembled an inverted 'V', thus lacking the cross-member, and had lower fitness than those networks that contained the cross member. The fitness of networks lacking the cross members ranged from 0.65-0.7, versus 0.85-0.9 for networks containing the cross member. This suggests that much of the functional behavior of the 'A' can be explained without the cross member, but that the cross member is necessary to fully explain the network's functional behavior.

Some links in the first Winslow's rhombus (Figure 8d) are unobservable. For example, the link that connects the middle input node to the bottom of the rhombus must be unobservable. If that link is removed and forces are instead applied to the bottom node of the rhombus, the reaction forces at the ground nodes will be identical to those that would result if the link were present. To see this, note that the vector sum of forces at the bottom node of the rhombus must equal the force carried in the unobservable link; otherwise, that node would not be in static equilibrium. Thus, the link does not contribute to the functional behavior of the network and is unobservable.

Some links in the second Winslow's rhombus (Figure 10d) also *appear* to be unobservable. The two diagonal links in that figure that are very faint never carried significant tension during a battery of tests that we applied. We did not test whether a significant shortening of those links in the target network resulted in an appearance of those links in the evolved networks.

The fitness function can affect the observability of links in the target network. Herein, we defined fitness to be a function of only the ground reaction forces. No topological or parameter comparisons were made. If, instead, the fitness of individuals depended on a comparison of the position of markers on the target network to the positions of markers on the individuals' networks, thereby adding a topological comparison, then the observability of the network could potentially increase.

Another concern is uniqueness of networks, as functionally equivalent networks with differing morphologies were found during our tests. For example, other networks that resemble the 'A' were found. They had similar topologies, in that all had diagonal outer members connected by a cross member, but the location of the cross member varied significantly. In the target network, the cross member connects to the bottom left node, yet in some evolved networks, it originated north of that node. The fitness appeared to be unaffected. In one case, the cross member bifurcated (see Figure 12). Thus, it would appear that multiple networks can have nearly equivalent functional behavior, despite their varied topologies.

4.2 Tests as Information

The fitness graphs shown in Figures 7, 9, and 11 are revealing. The population evolves until its maximum fitness reaches a plateau, and then another test is conducted on the target system. The test provides an additional data point to be explained by individuals in the GA population. In many cases, the maximum fitness of the population drops after the introduction of a new data point. In some cases, it drops precipitously. But in the case of Figure 11, the maximum fitness actually increases slightly after the introduction of certain tests.

The number of data points needed to discover the hidden network varied significantly. The 'A' network was often discovered by the GA after 9 or fewer tests while the Winslow's rhombus problems required 30 tests. The tests in the Winslow's rhombus problems were generated randomly and the tests used in

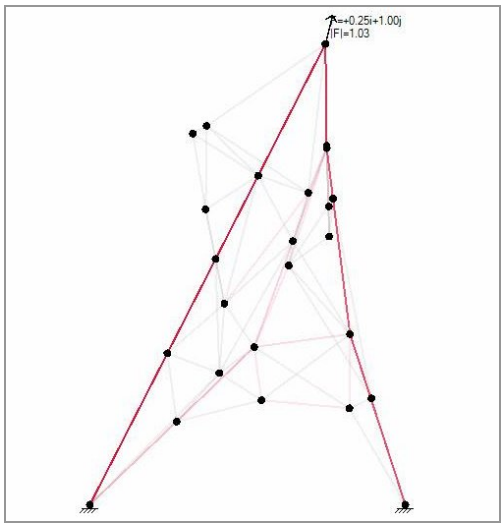

Figure 12. Evolved 'A' with bifurcated cross member

the 'A' problem were pre-specified. Yet in both cases, some tests did not cause a significant drop in population fitness.

This trend suggests that tests are a valuable source of information in system identification problems. A good test provides new data to be explained, and can therefore lower the fitness of existing individuals in the population. However, a poor test provides data similar to that already seen, and can therefore increase fitness.

Since one of our goals is to perform system identification using few tests on the target system and since good tests can yield more information than poor tests, we plan to co-evolve tests in future work. A good test will be one that discriminates between individuals in the population by maximizing the variance of their predictions. This approach has been successfully applied to other system identification problems [2], but never to the inference of cable network topology.

4.3 Subjective vs. Objective Fitness

The fitness measure used herein is subjective; fitness is based only on previously observed data from the target system. Because the fitness of a network individual is based only on limited observations, it may not reflect the true, or objective, fitness of the individual.

Defining objective fitness is a non-trivial problem in the case of network inference. One possible measure of objective fitness is the performance of the individual over a battery of exhaustive tests that are also performed on the target system. This type of fitness measures *functional equivalence;* it can be computationally expensive but is relatively straightforward to define. Another possible measure of objective fitness is *structural equivalence*, which compares the morphological equivalence of a network to the target network; structural equivalence is more difficult to define.

Direct measurement of objective fitness is usually impossible when attempting to identify real, physical systems. However, while working in simulation on test problems, defining and measuring objective fitness can provide valuable information about the performance of our method.

5. CONCLUSIONS AND FUTURE WORK

This paper described a genetic algorithm-based method for inferring networks using sparse data and few assumptions about network topology. The method alternates between testing the hidden network, and evolving new networks that can explain all previous tests on the hidden network.

We were able to infer a network that resembled the letter 'A', as well as two more complex networks based on a classical representation of the tendon network of a finger, known as Winslow's tendinuous rhombus.

We found that the quality of the evolved structures depended on the information gleaned from the tests performed on the target network. By maximizing the information from each test, we believe that we can minimize the number of tests required on the target network, as well as the time needed to evolve a network equivalent to the target.

In future work, we plan to apply co-evolution to the problem of generating good tests [2]. Ultimately, we plan to extend this method to the inference of anatomical structures, such as the tendon network of the human hand.

6. ACKNOWLEDGMENTS

This work was supported in part by the U.S. National Institute of Health (NIH), grant number 1-R01-AR052345-01.

7. REFERENCES

[1] Bongard, J. and Lipson, H., Automating Genetic Network Inference with Minimal Physical Experimentation Using Coevolution. In *Proceedings of the Genetic and Evolutionary Computation Conference*. Springer, 2004, 333-345.

[2] Bongard, J. and Lipson, H., Automating system identification using co-evolution of models and tests. *Evolutionary Computation*, (2005, In Press)

[3] D'haeseleer, P., Liang, S., and Somogyi, R., Genetic network inference: from co-expression clustering to reverse engineering. *Bioinformatics, 16, 8,* (2000), 707-726

[4] Gray, H. *Gray's Anatomy*. Senate, 1994.

[5] Iba, H., and Mimura, A., Inference of a gene regulatory network by means of interactive evolutionary computing. *Information Sciences, 145,* (2002), 225–236

[6] Lipson, H. A relaxation method for simulating the kinematics of compound nonlinear mechanisms*. ASME Journal of Mechanical Design*, (in review).

[7] Mahfoud, S.W. *Niching Methods for Genetic Algorithms.* Ph.D. Thesis, University Illinois at Urbana-Champaign, Urbana-Champaign, IL, 1995.

[8] Nelles, O. *Nonlinear System Identification: From Classical Approaches to Neural Networks and Fuzzy Models*. Springer, 2000.

[9] Overschee, P. and De Moor, B.L. *Subspace Identification for Linear Systems: Theory – Implementation – Applications*. Springer, 1996.

[10] Schoukens, J. and Pintelon, R. *Identification of Linear Systems*. Pergamon Press, 1991.

[11] Smith, V.A., Jarvis, E.D., and Hartemink, A.J., Evaluating functional network inference using simulations of complex biological systems. *Bioinformatics, 18, S1,* (2002), S216-S224.

[12] Zancolli, E., *Structural and Dynamic Bases of Hand Surgery*, 2nd ed., Lippincott, Philadelphia, PA, 1979.